

Radiative effects of aerosols on the evolution of the atmospheric boundary layer

Hongbin Yu, S. C. Liu,¹ and R. E. Dickinson

School of Earth and Atmospheric Sciences, Georgia Institute of Technology, Atlanta, Georgia, USA

Received 20 April 2001; revised 15 October 2001; accepted 18 October 2001; published 21 June 2002.

[1] This study investigates the impacts of tropospheric aerosols on the evolution of the atmospheric boundary layer (ABL) for dry subsiding regions by conducting simulations with a high-resolution ABL model. The scattering and absorption of aerosols diminish the surface radiation, inhibiting the sensible heat flux and evaporation and inducing feedbacks such as the enhanced stratification and change in relative humidity in the surface layer. The reduced sensible heat due to aerosol backscattering lowers the air temperature and suppresses the growth of the ABL. The resultant reduction of entrainment heating contributes to an additional cooling. The decreased entrainment drying competes with the reduced surface evaporation, so that the net effect can be either an increase or a decrease of the ABL moisture, depending on the soil moisture. Aerosol absorption decreases the turbulent heating but simultaneously increases the solar heating, increasing the air temperature and decreasing the strength of capping inversion. The resultant rise of the top of the ABL compensates the lowering due to the reduced buoyancy flux. With strong aerosol absorption, the increased entrainment heating enhances the ABL warming. Both the increased entrainment drying and the reduced evaporation decrease the ABL moisture. The increased warmth and dryness of the ABL imply that absorbing aerosols within the ABL decrease the probability of formation of boundary layer clouds, causing additional warming through cloud-feedbacks. The results are sensitive to the vertical distribution of absorbing aerosols. Absorbing aerosol above the ABL increases the strength of capping inversion and reduces the top of the ABL, hence decreasing the entrainment drying and moistening the ABL. *INDEX TERMS:* 3307 Meteorology and Atmospheric Dynamics: Boundary layer processes; 0305 Atmospheric Composition and Structure: Aerosols and particles (0345, 4801); 3322 Meteorology and Atmospheric Dynamics: Land/atmosphere interactions; 1620 Global Change: Climate dynamics (3309); *KEYWORDS:* Aerosols, atmospheric boundary layer, climate, radiation, atmospheric absorption

1. Introduction

[2] The atmospheric boundary layer (ABL) over the land is directly influenced by and rapidly responds to the diurnal cycle of solar radiation. Daytime solar radiation heats the surface, initiating thermal instability or convection. As the atmosphere is warmed through turbulent mixing, rising thermals penetrate to the overlying free troposphere and entrain the less turbulent overlying air. This entrainment of air with higher temperature and lower humidity into the turbulent ABL modifies the evolution of its thermal energy and moisture over the day [e.g., Garratt, 1992]. Under clear skies the daytime ABL, the so-called convective boundary layer, can extend to a height of 1–2 km or more. Strong turbulence homogenizes its conserved properties, that is, the potential temperature, specific humidity, and trace species like aerosols. Nighttime cooling of the surface by emission

of thermal infrared radiation stabilizes the near-surface air, forming a nocturnal inversion with a depth of the order of 100 m and a residual layer aloft. The ABL, through its controls on surface fluxes, is a major element of surface climatology, including the cycling of water and trace gases. Hence its investigation contributes to an understanding of near-surface temperature and humidities, cloudiness and precipitation, biogeochemical cycling, and levels of air pollution.

[3] The evolution of the ABL interacts directly with aerosols, modifying radiative fluxes by scattering and absorption of solar radiation and, to a lesser extent, by absorption and emission of thermal infrared radiation [Coakley *et al.*, 1983; Charlson *et al.*, 1992; Penner *et al.*, 1992]. Aerosols also affect radiation indirectly by acting as cloud condensation nuclei, leading to an increase in the number of cloud droplets and consequently in cloud reflectivity [Twomey, 1977], and a decrease in droplet size and hence an increase of cloud lifetime [Albrecht, 1989]. Aerosols and aerosol-affected clouds backscatter part of the solar radiation to space. Aerosols (with soot or mineral dust), alone or as part of cloud droplets, absorb part of the solar

¹Now at Institute of Earth Sciences, Academia Sinica, Taipei, Taiwan.

radiation and hence heat the surrounding atmosphere. Both the backscattering and the absorption reduce the solar radiation reaching the surface. The consequent perturbations of surface energy balance and atmospheric radiative heating alter the evolution of the ABL.

[4] Although the importance of aerosols for climate change has been widely recognized [*Intergovernmental Panel on Climate Change (IPCC)*, 1996], relatively little effort has been dedicated to investigating potential impacts of aerosols on the evolution of the ABL. “Nuclear winter” studies demonstrated that dust injected up to the stratosphere could influence the evolution of the ABL through reducing the net radiation at the surface [*Garratt et al.*, 1990]. Tropospheric aerosols, largely confined to the depth of the convective boundary layer, reduce radiative flux at the surface and simultaneously absorb the solar radiation in the atmosphere, hence significantly stratifying the atmosphere and inducing important feedbacks on the surface energy partitioning. In this study a high-resolution, one-dimensional (1-D) ABL model is used to (1) investigate the potential perturbations in the evolution of the ABL due to the direct effect of aerosols and (2) explore the implications for distributions of water vapor and air pollutants in the ABL. Although perhaps unrealistic in some aspects, such 1-D models provide high resolution and flexibility in conducting sensitivity studies, allowing the atmospheric response to radiative perturbations to be examined more easily than possible with complex three-dimensional models, and thus complementing and facilitating the interpretation of three-dimensional model results.

[5] The paper is organized as follows. Section 2 discusses major aspects of model simulations, including the ABL model, ambient environment and model parameters, and parameterizations of aerosol properties. The impacts of aerosols on the evolution of the ABL are presented and discussed in section 3. Specifically, discussed in section 3 are the effects of single-scattering albedo, optical depth, and vertical profile of aerosols, as well as soil moisture, subsidence, and duration of model simulations. Finally, major conclusions are summarized in section 4.

2. Description of Model Simulations

2.1. 1D ABL Model

[6] The response of ABL structure to the aerosol direct radiative perturbation is investigated with a modified version of the Coupled Atmosphere-Plant-Soil model (the so-called CAPS model). The CAPS model has been used as a stand-alone model for a number of numerical experiments under various geophysical conditions [e.g., *Ek and Mahrt*, 1991a, 1994; *Holtslag and Ek*, 1996; *Chang et al.*, 1999] and has also shown satisfactory overall performance when included in a number of research and operational three-dimensional large-scale models [e.g., *Holtslag et al.*, 1990; *Holtslag and Boville*, 1993; *Hong and Pan*, 1996]. Detailed description of the CAPS model is given by *Ek and Mahrt* [1991b] and *Chang et al.* [1999]. The following briefly reviews the major components of model physics and algorithms to facilitate later discussions.

[7] The CAPS model is a high-resolution ABL model with 70 layers, its first 46 model layers within the lowest

2 km at a resolution as fine as 20 m and a top level fixed at 10 km. The model treats turbulent mixing with a nonlocal K approach [*Troen and Mahrt*, 1986; *Holtslag and Moeng*, 1991] and its surface layer with Monin-Obukhov similarity. The depth of the ABL is diagnosed in terms of the modified bulk Richardson number with an inclusion of the temperature excess of thermals [*Troen and Mahrt*, 1986; *Holtslag and Boville*, 1993].

[8] The moisture and temperature within the soil layer are calculated by the diffusion equations for water and heat transport, respectively [*Mahrt and Pan*, 1984]. A surface energy balance module calculates the surface skin temperature and the potential evaporation (the maximum possible evaporation from a given surface of an environmental state) [*Ek and Mahrt*, 1991b; *Chang et al.*, 1999]. The evaporation from the surface is parameterized such that if the surface soil water content is greater than a specified lower limit of surface soil moisture, that is, the air-dry value [*Hillel*, 1982], evaporation proceeds at the potential rate (the so-called demand-control stage). Otherwise, the evaporation is proportional to the difference between the volumetric soil water content for the first soil layer and the specified air-dry value (the so-called flux-control stage) [*Mahrt and Pan*, 1984; *Chang et al.*, 1999].

[9] The oversimplified radiative scheme of CAPS [*Holtslag and van Ulden*, 1983; *Ek and Mahrt*, 1991b] has been replaced here by the so-called Fu-Liou broadband model [*Fu and Liou*, 1992, 1993; *Fu et al.*, 1997] that provides reasonable accuracy and compares well against a number of other radiative schemes [*Boucher et al.*, 1998; *Yu*, 2000].

2.2. Ambient Environment and Model Parameters

[10] Specified parameters were a solar orientation for 15 July at 40°N, clear sky conditions, a surface albedo of 0.2, and large-scale subsidence of 0.7 cm s⁻¹ above 2 km and decreasing linearly to 0 at the ground surface. The warming imposed by this subsidence depends in part on the temperature profiles. The initial lapse rate of temperature above 1 km was ~7 K km⁻¹. The wind speed was 2.7 m s⁻¹ at 20 m and 5 m s⁻¹ above 180 m and increased with height (z) as $z^{0.28}$ in between. For simplicity, the wind profile was fixed in the model calculation. A bare soil surface was considered, with texture arbitrarily chosen to be sandy loam, and with moisture content (the volumetric amount of liquid water in the soil, m³ m⁻³) saturated at 0.435, field capacity at 0.195, and air-dry value at 0.114 [*Ek and Mahrt*, 1994]. Soil moisture below the surface was held constant and hence not affected by surface fluxes. A volumetric water content was prescribed to be 0.18 and 0.22 in two layers centered at 0.05 and 0.5 m, respectively. Both condensation and precipitation were also assumed absent. These and other parameters and assumptions are changed later to evaluate the sensitivity of model results to them.

2.3. Inclusion of Aerosols

[11] Aerosol optical properties were specified using the optical depth, the single-scattering albedo (SSA), and the asymmetry factor, all functions of wavelength. The wavelength dependences of optical depth and asymmetry factor for a mixture of scattering and absorbing components can be described reasonably well by that for a purely scattering

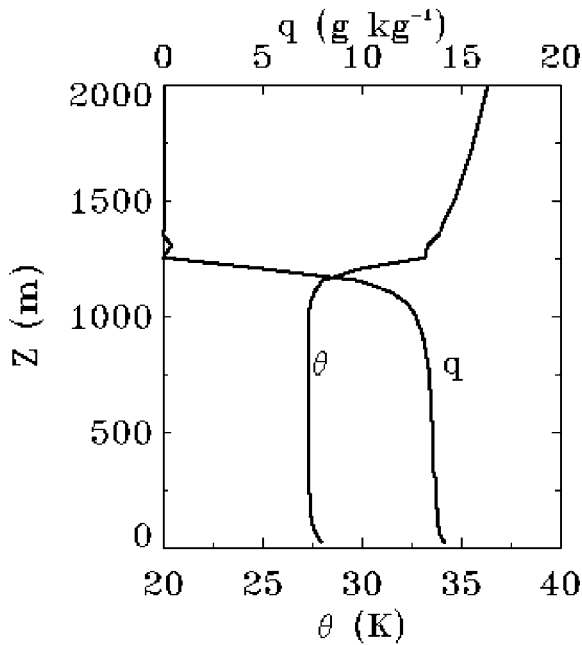


Figure 1. Profiles of potential temperature (θ) and specific humidity (q) at 1400 LST of day 40 for the aerosol-free experiment.

aerosol (e.g., sulfate) [Chylek *et al.*, 1995]. We parameterized these wavelength dependences on the basis of Mie calculations for sulfate aerosols at relative humidity (RH) of 70% [d'Almeida *et al.*, 1991]. The single-scattering albedo of tropospheric aerosols is uncertain and variable with variation from ~ 1.0 in the remote atmosphere to as low as 0.7 in highly polluted urban areas [Heintzenberg *et al.*, 1997; IPCC, 1994]. In addition, its dependence on wavelength involves the physical and chemical properties of aerosols [Chylek *et al.*, 1995].

[12] This study uses respective broadband values of the single-scattering albedo for the solar and thermal infrared wavelengths. The aerosol single-scattering albedo for solar flux was assumed to be 1.0, 0.9, and 0.8, to represent cases of pure scattering, moderate absorption, and strong absorption, respectively, whereas it was taken as 0.2 for thermal radiative flux. The latter assumption should not introduce any significant uncertainty because the optical depth in the thermal infrared is usually much smaller than that in the visible [Coakley *et al.*, 1983; Fouquart *et al.*, 1987]. The vertical distribution of aerosols was parameterized to be proportional to the calculated specific humidity, hence confining the aerosol to the boundary layer with a fairly

well-mixed distribution, consistent with aircraft measurements [Ching *et al.*, 1988].

3. Results and Discussion

[13] Two sets of simulations were run. Perturbation simulations with aerosols (i.e., a hazy atmosphere) are compared to control simulations that assume a clean atmosphere to obtain impacts of aerosols on the evolution of the ABL. The simulation time step is 3 and 12 min for ABL dynamics and atmospheric radiation, respectively.

3.1. Steady State ABL

[14] The model is run to near steady state, found to be approached after ~ 25 days of integration, corresponding to a 2-week damping time for temperature [Trenberth, 1992]. Figure 1 shows the simulated profiles of potential temperature and specific humidity at 1400 LST of day 40, typical of the convective boundary layer. The ABL height is ~ 1250 m.

[15] Table 1 lists the diurnal heat budgets in day 40 for the aerosol-free experiment. The whole system absorbs $\sim 370 \text{ Wm}^{-2}$ of solar radiation and is adiabatically heated by $\sim 95 \text{ Wm}^{-2}$, balanced by surface evaporative cooling and flux into soil of $\sim 180 \text{ Wm}^{-2}$ and thermal infrared cooling of $\sim 280 \text{ Wm}^{-2}$. Because of the assumption of a dry subsiding atmosphere, the latent flux is not put back into atmospheric heating. The apparently large flux into soil is related to the absence of vegetation cover and the simplification of the soil model (e.g., fixed soil temperature at the bottom and constant soil water content). Above 1.8 km the radiative cooling of $\sim 60 \text{ Wm}^{-2}$ is balanced mostly by adiabatic warming. Within the lowest 1.8 km the much higher water concentrations give the net radiative cooling of $\sim 100 \text{ Wm}^{-2}$, balanced approximately equally by adiabatic heating and surface sensible fluxes. With the balances imposed, the free atmosphere is closer to neutral stratification and the boundary layer on average is more stably stratified than given by average climatology. Since condensation and precipitation are not included, the water vapor distribution in the atmosphere is determined by a balance between the surface evaporation of $5.37 \text{ kg m}^{-2} \text{ d}^{-1}$ and the subsidence drying of $5.14 \text{ kg m}^{-2} \text{ d}^{-1}$.

[16] In summary, the examination of heat and moisture budgets clearly demonstrates that the day 40 simulation is near a steady state. In the following we will examine the impacts of aerosols on the evolution of the ABL on the basis of day 40 simulations. The transient response is also considered.

3.2. Aerosol-Radiation-ABL Interactions

[17] The aerosol optical depth at 550 nm was assumed to be 0.5, as commonly encountered over much of China

Table 1. Diurnal Heat Budgets for the Aerosol Free Experiment^a

System	SW	LW	AD	SH	ET	GH
0–1.8 km	51.5	–146.9	48.8	48.4	-	-
1.8–10 km	14.2	–58.8	46.9	-	-	-
Surface-atmosphere	370.6	–281.7	95.6	-	–159.5	–23.1

^aSW, LW, AD, SH, ET, and GH denote solar heating, thermal infrared cooling, adiabatic heating, sensible heating, evaporative cooling, and ground heat storage, respectively. According to the calculated ABL heights for both clean and hazy atmosphere, the altitude at 1.8 km is above the entrainment zone and is chosen as an approximate level dividing the ABL and the free atmosphere without calculations of entrainment heat flux. All terms are in a unit of Wm^{-2} .

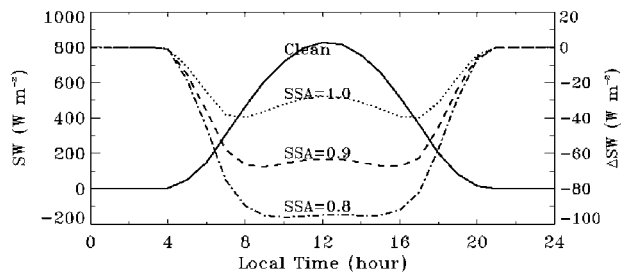


Figure 2. Diurnal variations of solar radiation absorbed by the surface for a clean atmosphere (solid line and left axis) and its perturbations (right axis) due to aerosols with different values of single-scattering albedo (SSA). Aerosol optical depth is 0.5 in the visible.

[Chameides *et al.*, 1999]. The columnar extinction was distributed in the vertical according to the calculated profile of specific humidity. The aforementioned three values of single-scattering albedo were employed to examine the role of aerosol absorption in affecting the evolution of ABL.

3.2.1. Perturbations in energy fluxes

[18] Aerosols substantially reduce the net solar flux absorbed by the surface, as shown in Figure 2, by more than 27 W m^{-2} for the purely scattering aerosols, with the largest reduction occurring in the early morning (0800 LST) and late afternoon (1700 LST). The diurnal variation of this reduction can be explained by the dependence of both aerosol upscattering fraction and Rayleigh scattering on the solar zenith angle [Nemesure *et al.*, 1995; Boucher *et al.*, 1998; Russell *et al.*, 1999]. The reduction in the surface net solar radiation increases with decreasing single-scattering albedo, because aerosol absorption removes part of solar radiation that would otherwise reach the surface. However, the solar radiation absorbed by aerosols leads to a significant ABL radiative heating, that is, an increase of about 5 and 8 K d^{-1} at noon for single-scattering albedo of 0.9 and 0.8, respectively. As discussed later, an excess of direct atmospheric heating will warm the ABL, affecting the surface energy partitioning and the ABL growth. Unlike that for purely scattering aerosols, perturbations of solar flux due to absorbing aerosols depend little on the solar zenith angle. The solar radiation absorbed by aerosols decreases with increasing solar zenith angle (SZA), compensating the SZA dependence of aerosol backscattering. How the reduction of solar flux at the surface changes with the SZA depends on such factors as aerosol type, aerosol amount, amount of absorption, Rayleigh scattering, and surface albedo.

[19] The perturbation in the incoming solar radiation changes the sum of the surface fluxes proportionally. Figure 3 shows changes in the sensible and latent heat flux, as well as the net available energy flux (a residue of the net radiative flux minus the ground heat flux). The reduction of latent heat flux is more than that of a sensible heat flux in the early morning and late afternoon and for purely scattering aerosols at times can exceed the change of net available energy flux with a corresponding increase of sensible flux by as much as 5 W m^{-2} (Figure 3a from 0700 to 1000 LST). In this situation, increases in relative humidities have decreased the atmospheric demand for water vapor by more

than the reduction in solar radiation, and sensible flux and surface-air temperature difference correspondingly increase. However, absorbing aerosols apparently always remove more than enough radiative energy from the surface to compensate for the reduction in evaporation, so that sensible fluxes always decrease, from the late morning to early afternoon more than the latent heat flux, and around noontime nearly compensating the reduction in available energy. Evaporation in the morning reduces the surface moisture below the air-dry value by around 1100 LST, after which it reaches a constant “saturation” level of $\sim 385 \text{ W m}^{-2}$ due to the fixed soil water content. The Bowen ratio (the ratio of the sensible to latent heat flux) averaged over 0800–1600 LST changes from 0.375 in the aerosol-free case to 0.380, 0.270, and 0.154 for single-scattering albedo of 1.0, 0.9, and 0.8, respectively. Exactly how latent and sensible fluxes are partitioned in response to the perturbations in the incoming radiation and surface layer properties will be sensitive to the specific land model and land cover assumed.

3.2.2. Perturbations in temperatures

[20] Figure 4 shows how the aerosol and its effects on the surface energy balance modify the surface skin temperature at equilibrium. The nighttime temperature is reduced by $\sim 1 \text{ K}$, consequent to the reduction of the surface solar heating

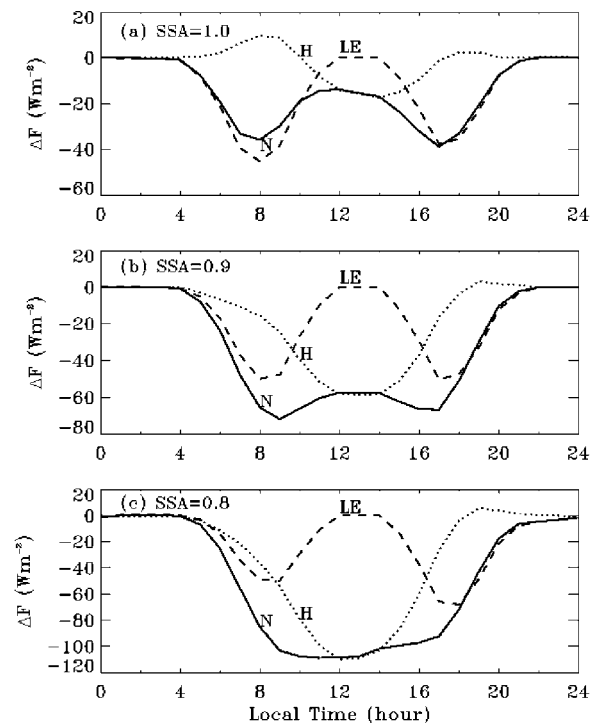


Figure 3. Aerosol-induced perturbations in net available energy flux (N, solid line), sensible heat flux (H, dotted line), and latent heat flux (LE, dashed line) for different values of single-scattering albedo: (a) SSA = 1.0; (b) SSA = 0.9; and (c) SSA = 0.8. Aerosol optical depth is 0.5 in the visible. Note that the latent heat flux perturbation vanishes around noontime because the surface moisture drops below the air-dry value in all cases and the evaporation is controlled by the prescribed soil water content.

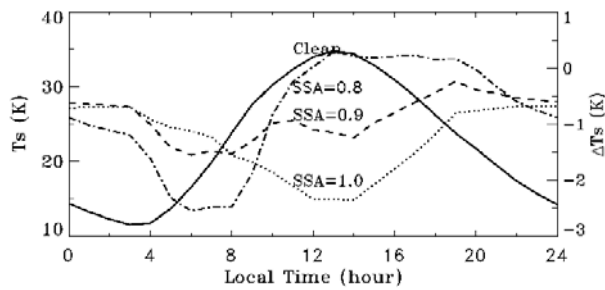


Figure 4. Diurnal variations of the surface skin temperature for a clean atmosphere (solid line and left axis) and its perturbations (right axis) due to aerosols with different values of single-scattering albedo (SSA). Aerosol optical depth is 0.5 in the visible.

in the previous day. After sunrise, temperatures decline more with the reduction of solar radiation. The nonabsorbing aerosol with its large evaporative cooling continues to reduce surface temperature later in the day (dotted line), but in the presence of absorbing aerosols (dashed and dot-dashed lines), the temperature reduction diminishes and even reverses sign by the afternoon for single-scattering albedo of 0.8. The sensible heat fluxes (Figure 3) are then reduced by more than enough to balance the reduction in the downward radiative fluxes (Figure 2) because of increased air temperature discussed in next paragraph.

[21] Figure 5 shows diurnal variations of air temperature at 2 m and its perturbations due to aerosols. Temperature at this level varies between the skin temperature and the ABL temperature. In the early morning the temperature in all cases is colder, following the decrease of the skin temperature. How the ABL temperature increases during the day depends on a balance between the surface sensible heat flux, the atmospheric absorbed solar radiation, and the entrainment heat flux at the top of ABL. Table 2 shows the aerosol-induced perturbations in these heat sources averaged over 0900–1500 LST. In the case of purely scattering aerosol, reductions in the sensible heating and the entrainment heating make comparable contributions to lowering the ABL temperature. The atmosphere absorbs a little less solar radiation because aerosols have backscattered some of the

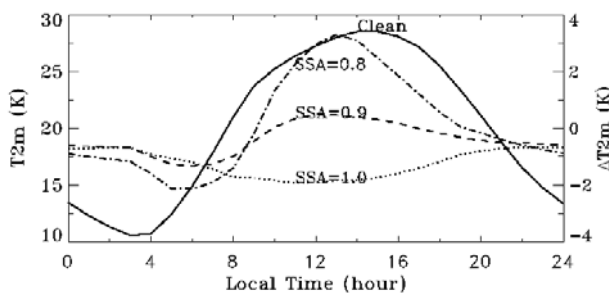


Figure 5. Diurnal variations of 2 m air temperature for a clean atmosphere (solid line and left axis) and its perturbations (right axis) due to aerosols with different values of single-scattering albedo (SSA). Aerosol optical depth is 0.5 in the visible.

Table 2. Aerosol-Induced Perturbations in ABL Solar Heating, Sensible Heating, and Entrainment Heating Averaged Over 0900–1500 LST for Different Values of Aerosol Single-Scattering Albedo^a

SSA	ΔSW	ΔSH	ΔQ_{ei}
1.0	-1.2	-8.5	-5.1
0.9	51.4	-50.0	-3.4
0.8	97.9	-94.6	+3.4

^a SSA, single-scattering albedo; ΔSW , ABL solar heating; ΔSH , sensible heating; ΔQ_{ei} , entrainment heating. All terms are in a unit of Wm^{-2} . Aerosol optical depth is 0.5 in the visible.

incoming solar radiation. When there is significant absorption in aerosols, the sensible heat flux decreases while the absorbed solar radiation increases, causing a net increase in ABL temperature. In the case of strongly absorbing aerosols (SSA = 0.8), the increased entrainment heating with elevation of the ABL (discussed later) enhances the ABL warming. When SSA is 0.9, in contrast, the entrainment heating is reduced and so the ABL warming.

[22] With their radiative forcing and consequent water vapor feedback, aerosols can either increase or decrease the diurnal temperature range (DTR), depending on their absorptive properties. The purely scattering aerosols reduce the DTR by ~ 1 K, but the absorbing aerosols increase it substantially, that is, by 1.3 and 4.6 K, for SSA of 0.9 and 0.8, respectively. Other factors not included in our model, for example, cloud feedbacks and changes in greenhouse gas concentrations, can also modify the DTR [Hansen et al., 1995; Stenchikov and Robock, 1995].

3.2.3. Perturbations in atmospheric stratification and ABL height

[23] How aerosols modify the stratification of the surface layer can be readily derived from differencing Figures 4 and 5. The larger the aerosol absorption, the larger the reduction in the surface-air temperature difference and the more stable the surface layer. With SSA = 0.8, the surface-air temperature difference decreases by as much as 3.5 K around noontime. Correspondingly, the Richardson number at that time changes from about -0.7 in the clean atmosphere to about -0.35 . This stabilization of the surface layer reduces the sensible heat flux and the surface evaporation (in the demand-control stage).

[24] Diurnal changes in the height of the ABL are determined by the surface buoyancy flux and the capping inversion, both of which are affected by aerosols. As shown in Figure 6, aerosols exert two pronounced impacts on the evolution of the ABL. First, it develops later and collapses earlier, by as much as ~ 2 hours, depending on the aerosol single-scattering albedo. Its growth and collapse are little affected by purely scattering aerosols because both the changes in the buoyancy flux and the strength of nocturnal inversion are small. However, with inhibition of the sensible heat flux and enhancement of the strength of nocturnal inversion by aerosol absorption, the ABL grows later and collapses earlier, the more so the stronger the absorption.

[25] Although a purely scattering aerosol lowers the top of the ABL, a strongly absorbing aerosol raises it. The percentage reduction in the accumulated buoyancy flux during the growth of the ABL is about 6.3, 32.0, and 53.5% for SSA of 1.0, 0.9, and 0.8, respectively. These

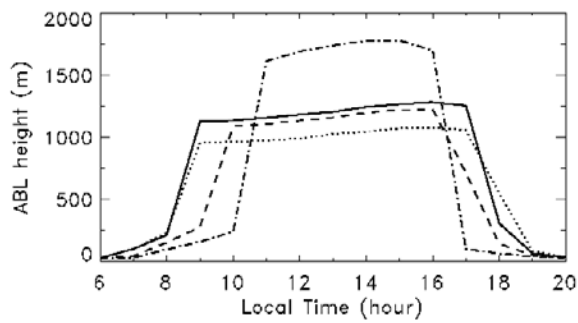


Figure 6. Diurnal variations of the ABL height for a clean (solid line) and hazy atmosphere with different values of aerosol single-scattering albedo (SSA): dotted line for SSA = 1.0; dashed line for SSA = 0.9; and dot-dashed line for SSA = 0.8. Aerosol optical depth is 0.5 in the visible.

alone cannot explain the change in the ABL height. The change in the strength of capping inversion also contributes. The purely scattering aerosols decrease the ABL temperature and enhance the capping inversion, hence further reducing the ABL height. In contrast, the absorbing aerosols by increasing the ABL temperature weaken the capping inversion, acting to cancel the effect of reduced buoyancy flux and raising the top of the ABL. In combination with the decrease in the buoyancy flux, the ABL height is kept nearly constant when SSA is 0.9 but is increased substantially when SSA is 0.8.

[26] Clearly, aerosols can alter the evolution of the ABL significantly and thus have important implications not only for the dynamics of ABL but also for air pollution properties. The resultant changes in the entrainment heating and drying can alter the heat and moisture budget in the ABL. The accumulation of air pollutants near the surface in the morning and later afternoon can be enhanced by aerosol heating. In addition, the fumigation of pollutants from the residual layer down to the convective ABL can be altered.

3.2.4. Perturbations in atmosphere moisture

[27] On a diurnal basis, the surface evaporation is reduced by about 8.5, 10.2, and 12.3% for SSA of 1.0, 0.9, and 0.8, respectively, and the daily water vapor content of the atmosphere is reduced by about 5.6, 8.6, and 8.1%, respectively. The corresponding reduction of water vapor content in the ABL is about 2.1, 20.0, and 34.3%. The specific humidity is proportional to this content divided by the thickness of the ABL. Figure 7 shows the diurnal variations of the ABL-averaged specific humidity and its perturbations due to aerosols. In the purely scattering case the reduction in the entrainment drying of -18.3 Wm^{-2} exceeds the reduction in the surface evaporation of -8.3 Wm^{-2} , leading to an increase in the specific humidity. In the absorbing cases the later growth and earlier decay of the ABL promotes greater specific humidities earlier and later in the day. However, at midday, the reduced evaporation, the greater height of the ABL, and increased entrainment all contribute to reduction of the specific humidities. On a daily basis the increased entrainment drying (2.0 and 44.7 Wm^{-2} for SSA = 0.9 and 0.8, respectively), along with the reduced surface evaporation (-12.5 and -14.0 Wm^{-2} , correspondingly), decreases the average specific humidity. The

increase of entrainment drying for SSA of 0.8 contributes about a factor of 3 more than the decrease of surface evaporation.

[28] The aerosol-induced decrease in the water vapor content alters the radiative effects of water vapor and hence the temperature. Calculations show that a 10% decrease of the water vapor content reduces the downward radiation reaching the surface by $\sim 5 \text{ Wm}^{-2}$ at night but by only 1.5 Wm^{-2} during the daytime, when the decreased greenhouse effect is countered by an increase in the downward solar radiation. Consequently, although this water vapor feedback contributes to the decrease of $\sim 0.5 \text{ K}$ for the surface skin temperature and 2 m air temperature at night, its effect on daytime temperatures is negligible.

[29] Changes in the RH near the surface and near the top of ABL, depending on changes of temperature and specific humidity, are shown in Figure 8. The RH near the surface is increased by $\sim 10\%$ for purely scattering aerosol, while it is reduced for the absorbing aerosol. For strongly absorbing aerosols this reduction can be as large as 25%. The changes of RH that depend on the degree of aerosol absorption in turn modify the surface evaporation, as discussed earlier. Probability of fog formation that depends on relative humidity will increase for scattering aerosol but decrease with sufficient absorption. In addition, aerosols may change atmospheric circulations and hence affect the formation of advective fog.

[30] The RH is maximum near the top of the ABL and hence is a measure of the probability of ABL cloud formation. As shown in Figure 8b, the purely scattering aerosols increase this maximum RH by more than 10% and hence the probability of cloud formation. On the other hand, the absorbing aerosols with their reduction of RH reduce the probability of cloud formation. Since all observed aerosols are at least moderately absorbing, our results are consistent with the recent cloud-burning observations related to absorbing aerosols [Ackerman *et al.*, 2000]. Soot in highly polluted areas such as China should cause a warming effect through the cloud feedbacks (the so-called semidirect effect) [Hansen *et al.*, 1997], in addition to that due to aerosol absorption.

3.2.5. Heat budget

[31] As a summary of aerosol-radiation-ABL interactions, we examine the perturbations in the heat budget.

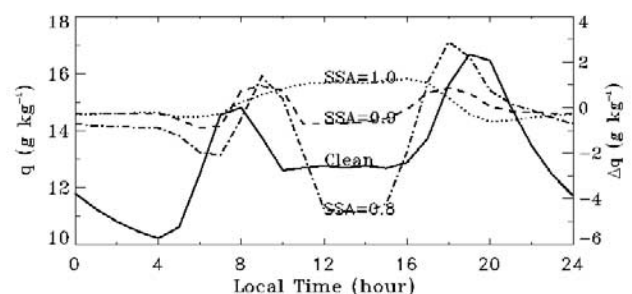


Figure 7. Diurnal variations of the ABL-averaged specific humidity for a clean atmosphere (solid line and left axis) and its perturbations (right axis) due to aerosols with different values of single-scattering albedo (SSA). Aerosol optical depth is 0.5 in the visible.

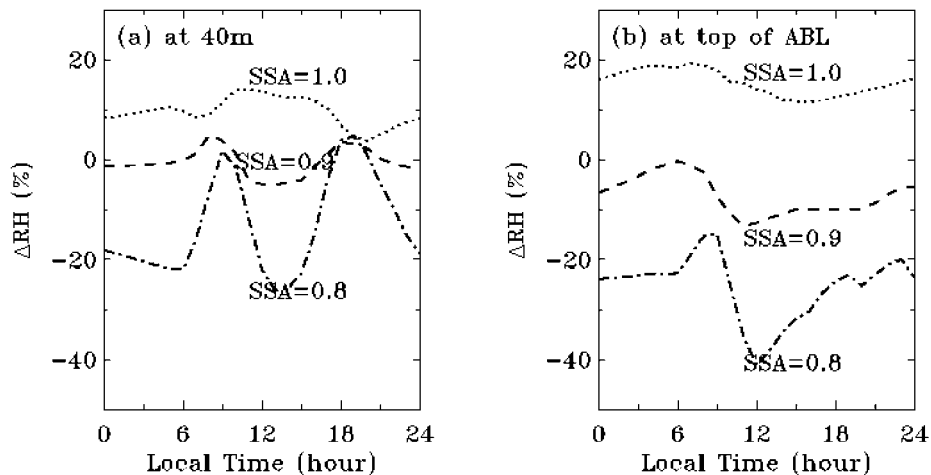


Figure 8. Aerosol-induced perturbations in the relative humidity (RH) (a) at 40 m and (b) near the top of ABL for different values of single-scattering albedo (SSA). Aerosol optical depth is 0.5 in the visible.

Table 3 lists the daily averaged heat budget for the tropospheric air. Aerosol scattering and absorption of solar radiation decrease the surface sensible heat flux and hence the heat input to the atmosphere. This decrease in the sensible heat flux becomes much larger when the single-scattering albedo decreases from 1.0 to 0.8. Although the solar flux decreases for purely scattering, with any absorption it will increase. The thermal infrared cooling changes much less, especially for absorbing aerosols. The gradient of potential temperature changes with aerosol effects, perturbing the adiabatic heating due to the subsidence. For the prescribed vertical motion the adiabatic heating is proportional to the change of potential temperature between the mixed layer and the model top. The purely scattering aerosol increases the adiabatic heating somewhat, but for absorbing aerosols the adiabatic heating is decreased substantially and counters the additional solar heating, that is, by about 17 and 30% for SSA of 0.9 and 0.8, respectively.

[32] The perturbation in the heat budget of the surface-atmosphere system is shown in Table 4. For the purely scattering aerosol, a decrease of $\sim 20 \text{ Wm}^{-2}$ in the solar radiative flux is largely balanced by a decrease in the surface evaporative cooling (59%), an increase in the adiabatic heating (17%), and a decrease in the thermal infrared cooling (14%). Aerosol absorption acts to cancel the cooling by aerosol backscattering. The total reduction in

the sum of the radiative and adiabatic heating is largely balanced by the decrease in the surface evaporative cooling.

[33] Clearly, how aerosols perturb the heat and moisture budgets and the evolution of ABL depends on aerosol absorption. With pure scattering, they cool and humidify the ABL, while with absorption they warm and dry it. The sensitivity of aerosol-induced ABL perturbations to various additional parameters is now examined, including soil moisture, subsidence, aerosol optical depth, aerosol profile, and duration of model simulations.

3.3. Effects of Soil Moisture

[34] The volumetric water content was increased by 0.04 for the two model soil layers to test the sensitivity of the above results to the soil moisture. This test is denoted the wet-soil case, and the previous case as the dry-soil case. Other ambient conditions were kept the same. For the wet-soil case, surface evaporation always proceeds at the potential rate, with a peak of $\sim 525 \text{ Wm}^{-2}$ at noon, which is substantially larger than the saturation level of 385 Wm^{-2} in the dry-soil case. Correspondingly, the maximum sensible heat flux is less in the wet-soil case (135 Wm^{-2}) than in the dry-soil case (225 Wm^{-2}).

[35] Figure 9 shows for the wet-soil case perturbations in the surface fluxes due to aerosol-radiation interactions that differ significantly from those in Figure 3. The demand-

Table 3. Aerosol Induced Perturbations in the Daily Averaged Heat Budget of the 0–10 km Atmosphere for Different Values of Aerosol Single-Scattering Albedo^a

SSA	ΔSW	ΔLW	ΔAD	ΔSH
1.0	-0.9	-1.3	3.5	-2.0
0.9	24.1	-2.8	-4.5	-17.9
0.8	46.0	-1.1	-14.0	-33.2

^aSW, LW, AD, and SH denote solar heating, thermal infrared cooling, adiabatic heating, and sensible heating, respectively. All terms are in a unit of Wm^{-2} . Aerosol optical depth is 0.5 in the visible.

Table 4. Aerosol-Induced Perturbations in the Daily Averaged Surface-Atmosphere Heat Budget for Different Values of Aerosol Single-Scattering Albedo^a

SSA	ΔSW	ΔLW	ΔET	ΔAD	ΔGH
1.0	-20.4	2.8	12.1	3.5	-0.1
0.9	-10.8	-1.4	14.9	-4.5	0.2
0.8	-2.5	-2.5	17.3	-14.0	-0.5

^aSW, LW, ET, AD, and GH denote solar heating, thermal infrared cooling, evaporative cooling, adiabatic heating, and ground heat storage, respectively. All terms are in a unit of Wm^{-2} . Aerosol optical depth is 0.5 in the visible.

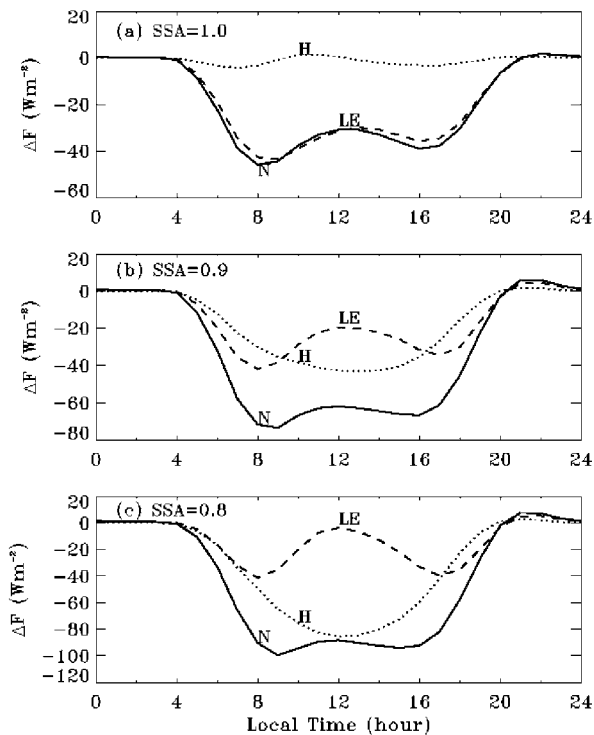


Figure 9. Aerosol-induced perturbations in net available energy flux (N, solid line), sensible heat flux (H, dotted line), and latent heat flux (LE, dashed line) in the wet-soil case and for different values of single-scattering albedo: (a) SSA = 1.0; (b) SSA = 0.9; and (c) SSA = 0.8.

control evaporation can change in response to the perturbations in both the incoming solar radiation and the surface layer requirement for sensible fluxes, contrary to the dry-soil case, in which the flux-control evaporation around noontime does not respond to these perturbations. For purely scattering aerosol the reduction in the net available radiative flux largely goes to reducing the evaporation because of the negligible changes in the surface-air temperature difference. The drier air with absorbing aerosols increases the atmospheric demand for the water vapor, compensating the reduced evaporation due to the cooling effect of decreased radiative flux and resulting in a small change in the latent heat flux during most daylight hours.

[36] The reduction in the accumulated buoyancy flux is about 4.0, 32.0, and 55.8% for SSA of 1.0, 0.9, and 0.8, respectively, not significantly different than that in the dry-

soil case. However, the reduction in the daily surface evaporation now is less with increasing aerosol absorption, namely, 10.6, 9.2, and 8.4% for SSA of 1.0, 0.9, and 0.8, respectively. Table 5 lists the perturbation in the diurnal heat budget for the surface-atmosphere system in the wet-soil case. Evaporative cooling is reduced more with purely scattering aerosols but less with strongly absorbing ones. Consequently, for strongly absorbing aerosols, the increase in ABL temperature and reduction in adiabatic heating are less. For purely scattering aerosols the decrease in ABL temperature and increase in adiabatic heating are less. When aerosol single-scattering albedo is 0.9, there is little difference between the two cases.

[37] Similar to the dry-soil case, absorbing aerosols can delay the growth and promote the collapse of the ABL. However, the equilibrium ABL height in the strongly absorbing case no longer increases significantly as it did for the dry-soil case. The major contributing factor to the difference is the small ABL warming in the wet-soil case, hence little change in the strength of capping inversion.

[38] Table 6 shows the perturbations in the surface evaporation and in the entrainment drying flux. Aerosols dry out the ABL for the wet-soil regardless of their absorption, in contrast to the dry-soil. The resultant change in the specific humidity around noontime is about -0.5 , -0.7 , and -1.1 g kg^{-1} for SSA of 1.0, 0.9, and 0.8, respectively. Surface evaporation is reduced more for the wet-soil purely scattering aerosols, but in the strongly absorbing case a much smaller increase in the entrainment drying reduces the ABL drying. Hence, overall, the dependence on aerosol absorptive properties is less. Figure 10 shows changes in the RH at 40 m and the maximum RH near the top of ABL. In comparison to Figure 8 the changes in the RH at 40 m are generally smaller, a result of the smaller perturbations in the temperature and moisture. Near the top of ABL, the RH now changes little for pure scattering, but in contrast to RH at 40 m, the strongly absorbing aerosol changes RH and consequences for cloud formation are similar.

3.4. Effects of Subsidence

[39] The evolution of the ABL depends on the properties of the free atmosphere. Changes in the subsidence and/or the profiles of potential temperature and moisture will alter the ABL heat and moisture budget. The subsidence was changed from 0.7 cm s^{-1} to 1 cm s^{-1} , but other ambient conditions were kept the same as in section 3.2. This increase in the subsidence increases the atmospheric adiabatic heating by $\sim 12.6\%$. The ABL height and ABL-averaged potential temperature change significantly, that

Table 5. Aerosol-Induced Perturbations in the Daily Averaged Surface-Atmosphere Heat Budget in the Wet-Soil Case for Different Values of Aerosol Single-Scattering Albedo^a

SSA	ΔSW	ΔLW	ΔET	ΔAD	ΔGH
1.0	-20.7	1.0	17.7	-0.2	0.04
0.9	-10.9	-1.5	15.1	-4.6	0.4
0.8	-2.7	-4.3	13.1	-9.4	-0.4

^a SW, LW, ET, AD, and GH denote solar heating, thermal infrared cooling, evaporative cooling, adiabatic heating, and ground heat storage, respectively. All terms are in a unit of Wm^{-2} . Aerosol optical depth is 0.5 in the visible.

Table 6. Aerosol-Induced Perturbations in the Surface Evaporation and in the Entrainment Drying Averaged Over 0900–1500 LST in the Wet-Soil Case and for Different Values of Aerosol Single-Scattering Albedo^a

SSA	ΔQ_{q0}	ΔQ_{qi}	$\Delta Q_{q0} - \Delta Q_{qi}$
1.0	-33.9	-15.0	-18.9
0.9	-23.7	-2.1	-21.6
0.8	-12.6	+6.9	-19.5

^a ΔQ_{q0} , surface evaporation; ΔQ_{qi} , entrainment drying. The fluxes have a unit of Wm^{-2} . Aerosol optical depth is 0.5 in the visible.

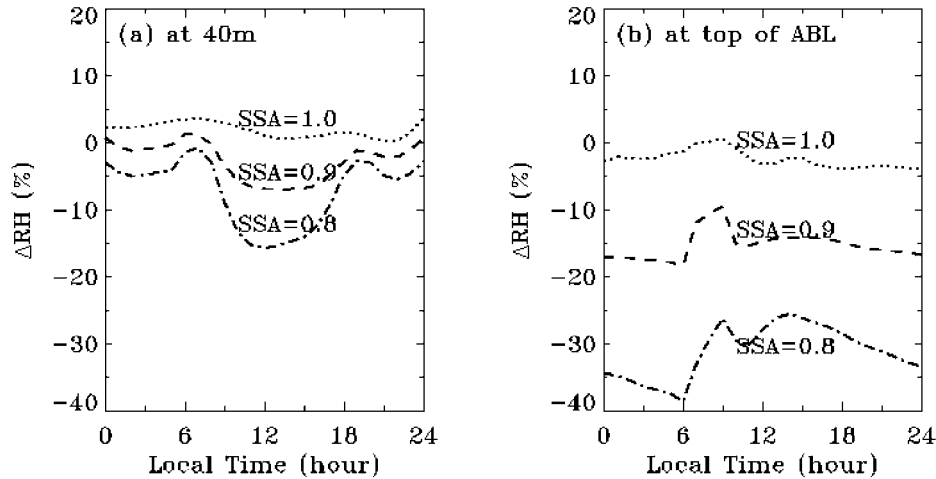


Figure 10. Aerosol-induced perturbations in the relative humidity (RH) (a) at 40 m and (b) near the top of ABL for different values of single-scattering albedo (SSA) and for the wet-soil case.

is, 870 m and 30.5 K at 1400 LST, compared to 1250 m and 27.5 K for the subsidence of 0.7 cm s^{-1} . The change of specific humidity is small, and the relative humidity decreases. The increased subsidence decreases the total water vapor content by $\sim 28\%$.

[40] Perturbations induced by the purely scattering aerosol are not sensitive to the subsidence. For the strongly absorbing aerosols the change of adiabatic heating is largely compensated by a change in radiative cooling and surface energy terms change less, as shown in Table 7. The inversion strength decreases less, the top of the ABL is lower, and the ABL humidity decreases less in the case of stronger subsidence. However, the major results of aerosol-radiation-ABL interactions discussed in section 3.2 do not change.

3.5. Effects of Aerosol Optical Depth

[41] Initial and boundary conditions are specified as in section 3.2, but CAPS is run with different aerosol optical depths. Both the reduction in the surface solar radiation and the enhanced solar heating due to aerosol absorption increase with increasing optical depth, hence also the perturbations in the ABL temperature and moisture, as shown in Figure 11 for the air temperature at 2 m and at noon.

[42] The size of particles and hence their optical properties depend on the relative humidity. The optical properties have been previously prescribed. Here we examine how changes in relative humidity due to radiative effects of

aerosols would modify aerosol optical properties and further affect the evolution of the ABL. For a constant aerosol mass loading of 0.05 gm^{-2} , we parameterized the RH dependence of scattering coefficient on the basis of *Kiehl and Briegleb* [1993]. The absorption coefficient of aerosols was not allowed to change with RH. Figure 12 shows changes of air temperature at 2 m with and without an inclusion of RH feedbacks. For purely scattering aerosols the air temperature is reduced by more than 25% when including the RH feedback, because of the large increase in relative humidity compared to the clean atmosphere, and hence aerosol extinction. However, for absorbing aerosols the decrease in the humidity reduces both the extinction and the single-scattering albedo of aerosols. The two effects compensate each other, and the net effect can be either positive or negative, depending on time of day and also variables. To make things more complicated, the RH dependence of aerosol properties is strongly nonlinear and composition-dependent, suggesting that different feedbacks could result for different ambient conditions and aerosol compositions.

3.6. Effects of Aerosol Profile

[43] Although the surface radiative perturbation is expected to be less sensitive to the vertical distribution of aerosols than to its optical depth, the vertical distribution of the perturbed radiative heating rate in the ABL depends strongly on the profile of absorbing aerosols. In the above simulations (denoted as q profile cases, for convenience), the q -based parameterization confined aerosols to a fairly

Table 7. Aerosol-Induced Percentage Perturbations in the Daily Averaged Heat Budgets for Different Values of Subsidence^a

Subsidence, cm s^{-1}	0–10 km Atmosphere				Surface-Atmosphere System				
	ΔSW	ΔLW	ΔAD	ΔSH	ΔSW	ΔLW	ΔET	ΔAD	ΔGH
1.0	73.1	-3.2	-8.0	-66.3	-0.7	-2.3	11.5	-8.0	3.2
0.7	70.0	-0.5	-14.6	-68.6	-0.7	-0.9	10.8	-14.6	-2.2

^aSW, LW, AD, SH, ET, and GH denote solar heating, thermal infrared cooling, adiabatic heating, sensible heating, evaporative cooling, and ground heat storage, respectively. Aerosol optical depth is 0.5 in the visible, and the single-scattering albedo is 0.8.

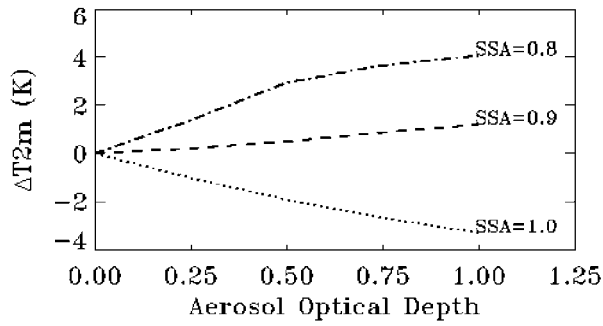


Figure 11. Changes of air temperature at 2 m and at noon as a function of aerosol optical depth for different values of aerosol single-scattering albedo (SSA).

well-mixed ABL. In the following the constant aerosol optical depth of 0.5 is uniformly distributed in a time-independent layer with a nominal mixing height (H_{aer}) of 1 km or 2 km, similar to those employed in some three-dimensional studies [e.g., *Kiehl and Briegleb, 1993*]. Other

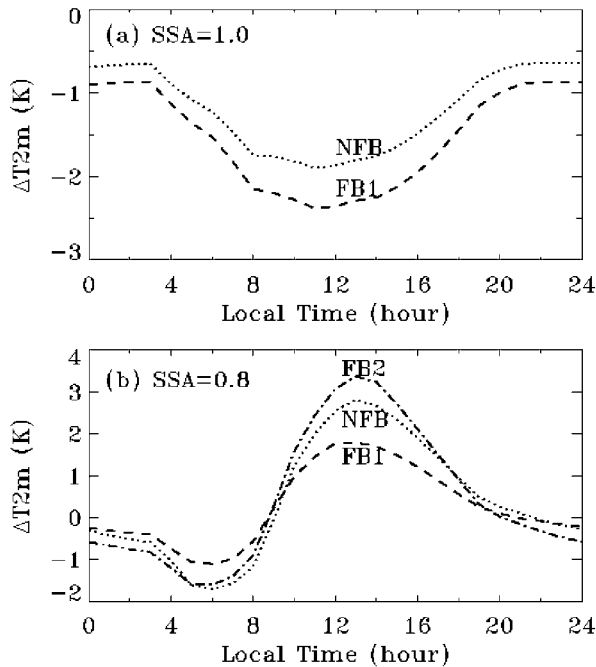


Figure 12. Changes of air temperature at 2 m by aerosol mass loading of 0.05 gm^{-2} for (a) $\text{SSA} = 1.0$ and (b) $\text{SSA} = 0.8$. A dependence of aerosol scattering coefficient on relative humidity is parameterized according to *Kiehl and Briegleb* [1993]. Symbol NFB denotes a simulation without RH feedback in which the hourly relative humidity for a clean atmosphere is used. Symbol FB1 denotes a simulation in which the effect of relative humidity on the optical depth is considered, while FB2 denotes a simulation with a consideration of the effects of relative humidity on both the optical depth and single-scattering albedo.

Table 8. Aerosol-Induced Perturbations in the ABL-Averaged Potential Temperature, the Potential Temperature in the Overlying Free Troposphere, the Daytime Accumulated Buoyancy Flux, and the Equilibrium ABL Height for Different Values of Aerosol Single-Scattering Albedo and Aerosol Mixing Height^a

H_{aer}	SSA	$\Delta \theta_{\text{ABL}}, ^\circ\text{C}$	$\Delta \theta_{\text{FT}}, ^\circ\text{C}$	$\Delta B, \%$	$\Delta h, \text{m}$
1 km	0.9	+1.0	+0.2	-30.5	-10
1 km	0.8	+5.0	-1.8	-59.7	+1700
2 km	0.9	-0.5	+2.5	-29.8	-320
2 km	0.8	+0.5	+5.0	-54.1	-440

^a $\Delta \theta_{\text{ABL}}$, ABL-averaged potential temperature; $\Delta \theta_{\text{FT}}$, potential temperature in the overlying free troposphere; ΔB , daytime accumulated buoyancy flux; Δh , equilibrium ABL height; H_{aer} , aerosol mixing height. Aerosol optical depth is 0.5 in the visible.

ambient conditions are kept the same as that in section 3.2. Under this assumption, the smaller the aerosol mixing height, the larger the near-surface solar heating rate becomes. Conversely, more aerosols would reside in and hence heat the overlying free troposphere for larger mixing height (e.g., $H_{\text{aer}} = 2 \text{ km}$). It is thus expected that the profiles of absorbing aerosols can potentially affect the evolution of the ABL.

[44] The downward radiative flux is reduced more in the $H_{\text{aer}} = 1 \text{ km}$ case than in the $H_{\text{aer}} = 2 \text{ km}$ case, resulting mainly from different perturbations in the thermal infrared flux. The difference between the two cases can be as large as $\sim 20 \text{ Wm}^{-2}$ in the morning for SSA of 0.8. Even larger differences exist in the reduction of sensible heat flux. The larger the fraction of the aerosol that is within the mixed layer, the larger the reduction in the sensible heat because of the larger solar heating in the ABL and hence reduced surface-air temperature difference. In the case of $\text{SSA} = 0.8$, the reduction in the sensible heat flux around noontime is $\sim 55 \text{ Wm}^{-2}$ larger for $H_{\text{aer}} = 1 \text{ km}$ than for $H_{\text{aer}} = 2 \text{ km}$.

[45] Table 8 compares for different aerosol profiles the changes in the ABL-averaged potential temperature and the potential temperature in the overlying free troposphere at 1400 LST, the daytime accumulated buoyancy flux, and the equilibrium ABL height. Although there are no significant deviations in the reduction of the accumulated buoyancy

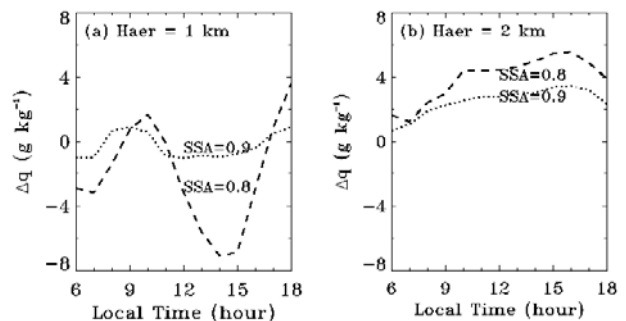


Figure 13. Aerosol-induced perturbations in the specific humidity for different values of aerosol single-scattering albedo (SSA) and aerosol mixing height (H_{aer}): (a) $H_{\text{aer}} = 1 \text{ km}$ and (b) $H_{\text{aer}} = 2 \text{ km}$.

Table 9. Aerosol-Induced Perturbations in the Surface Evaporation and in the Entrainment Drying Averaged Over 0900–1500 LST for Different Values of Aerosol Single-Scattering Albedo and Aerosol Mixing Height^a

H_{aer}	SSA	ΔQ_{q0}	ΔQ_{qi}	$\Delta Q_{q0} - \Delta Q_{qi}$
1 km	0.9	-12.8	-5.2	-7.6
1 km	0.8	-15.5	+135.2	-150.7
2 km	0.9	-13.3	-38.6	+25.3
2 km	0.8	-21.5	-89.1	+67.6

^aThe fluxes have a unit of Wm^{-2} . Aerosol optical depth is 0.5 in the visible.

flux, changes in the ABL height depend strongly on aerosol profiles, largely due to different perturbations in the strength of capping inversion. When absorbing aerosols are confined to the ABL (i.e., $H_{\text{aer}} = 1$ km and q profile cases), the reduced strength of capping inversion causes a small reduction in the ABL height when $\text{SSA} = 0.9$ and a significant increase in the ABL height when $\text{SSA} = 0.8$. For $H_{\text{aer}} = 2$ km, a large part of aerosol resides above the perturbed ABL, increasing the temperature of the overlying air significantly, but temperature of the ABL is increased less or even decreased. Consequently, the strength of

capping inversion increases, and the top of the ABL is substantially lowered. The perturbation in the entrainment heat flux also depends on aerosol profiles. In the case of $H_{\text{aer}} = 1$ km and $\text{SSA} = 0.8$, the entrainment heat flux increases by about 17 Wm^{-2} , that is, much larger than a 3.4 Wm^{-2} in the q profile case (see Table 2). In the case of $H_{\text{aer}} = 2$ km, however, the entrainment flux decreases by about 9.3 and 12.4 Wm^{-2} for SSA of 0.9 and 0.8, respectively.

[46] The change in the specific humidity is illustrated in Figure 13. When $H_{\text{aer}} = 1$ km, the reduction in the specific humidity is similar to but slightly larger than that discussed in section 3.2. On the other hand, in the case of $H_{\text{aer}} = 2$ km, the specific humidity goes the other direction, that is, increases significantly. Changes of humidity are closely related to changes in entrainment drying, as illustrated in Table 9. In the case of $H_{\text{aer}} = 1$ km and $\text{SSA} = 0.8$, the entrainment drying increases significantly due to a large rise of the top of ABL, decreasing the ABL humidity by as much as 7 g kg^{-1} in the afternoon. In the case of $H_{\text{aer}} = 2$ km, in contrast, the reduced entrainment drying dominates over the reduced evaporation, giving rise to the net increase in the specific humidity.

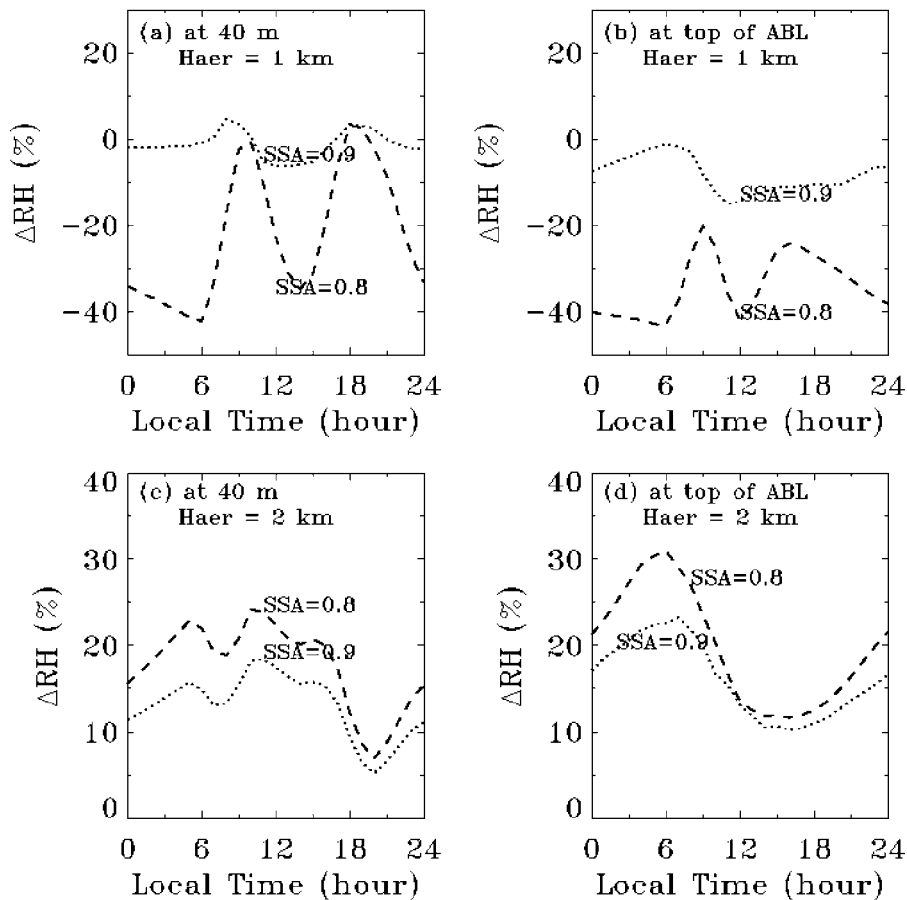


Figure 14. Aerosol-induced perturbations in the relative humidity (RH) (a and c) at 40 m and (b and d) near the top of the ABL for different values of aerosol single-scattering albedo (SSA) and aerosol mixing height (H_{aer}): (a and b) $H_{\text{aer}} = 1$ km and (c and d) $H_{\text{aer}} = 2$ km.

Table 10. Changes of Sensible Heat Flux, 2m Air Temperature, and the ABL-Averaged Specific Humidity at Noon for Days 2, 5, and 40^a

	Day 2	Day 5	Day 40
ΔH (Wm^{-2})	-85	-92	-100
ΔT_{2m} (K)	1.0	2.3	2.7
Δq (g kg^{-1})	-0.8	-2.0	-2.0

^a ΔH , sensible heat flux; ΔT_{2m} , 2m air temperature; Δq , ABL-averaged specific humidity. Aerosol optical depth is 0.5, and single-scattering albedo is 0.8 in the visible.

[47] Figure 14 shows the changes in the relative humidity. When $H_{\text{aer}} = 1$ km and $\text{SSA} = 0.8$, reduction in the RH is somewhat larger than that discussed in section 3.2, because of the larger reduction in the specific humidity and the larger ABL warming. In the case of $H_{\text{aer}} = 2$ km, however, the RH increases significantly due to the increased specific humidity and the smaller ABL warming. Evidently, depending on whether or not absorbing aerosols such as smoke from biomass burning and mineral aerosol from a dust storm are largely within the ABL, the probability of formation of boundary layer clouds can either decrease or increase.

3.7. Effects of Duration of Model Simulations

[48] Meteorological variability will affect aerosol loading, changing its optical depth from day to day. To examine potential impacts of the assumption of steady state, we simulate a case of temporal variation of aerosol optical depth with an idealized 1-week cycle starting from day 1. During a 1-week period, aerosols undergo a linear buildup stage (3 days), then a maintenance stage (3 days), and finally a linear depletion stage (1 day). The calculations show that the perturbations in the case of constant aerosol optical depth are somewhat larger than that in the varying optical depth case, with the largest differences around noontime usually $<25\%$. Therefore fluctuations in the aerosol optical depth should not significantly alter the findings discussed earlier.

[49] Sensitivity tests show that the transient perturbations are not sensitive to initial ABL temperature profiles. However, they could depend strongly on the initial moisture profiles in the case of absorbing aerosols, because the

vertical distributions of aerosols in the simulations have been parameterized on the basis of those of moisture. Table 10 compares surface and ABL properties at day 2 and 5 with day 40, when aerosol profiles do not change significantly during the simulation. By day 5 or even earlier, the perturbations are already close to steady state.

4. Summary and Conclusions

[50] Through their scattering and absorption, aerosols reduce the solar radiation reaching the surface, a part of which reduction can be absorbed in the atmosphere. Such reduction and redistribution of the radiative heating can impact the ABL. In this study we have conducted simulations with a high-resolution ABL model to investigate these impacts. Major perturbations induced by the ABL aerosols are summarized in Table 11 and in the following.

[51] With decreased solar radiation at the surface, the sum of the sensible and latent heat fluxes also decreases and induces important feedbacks. The ABL can either be moistened, as for purely scattering aerosol, or be dried, as for absorbing aerosols, hence either suppressing or promoting evaporation. Aerosol absorption reduces the surface-air temperature difference and hence sensible heat fluxes. The partitioning of energy between sensible heat fluxes and evaporation depends not only on this absorption but also on the soil moisture.

[52] If sensible heat fluxes are reduced, so is the heating of the overlying atmosphere. However, aerosols directly heat the atmosphere by absorption. Thus, if purely scattering, aerosols reduce the temperature of the ABL, but with strong absorption, increase it. The average heat gain or loss induced by these perturbations is balanced mostly by changes of the adiabatic heating. In addition, entrainment heating also contributes during daytime, either positively for strongly absorbing aerosols or negatively for purely scattering aerosols.

[53] Aerosols alter the growth of ABL by changing both the surface buoyancy flux and capping inversion. A reduction in surface buoyancy flux delays growth and promotes collapse of the ABL. The reduced ABL temperature along with the reduced buoyancy flux in the purely scattering case increases the strength of capping inversion, lowering the top

Table 11. Summary of Major ABL Perturbations Induced by Purely Scattering and Strongly Absorbing Aerosols Within the ABL^a

ABL Parameters	Purely Scattering Aerosols	Strongly Absorbing Aerosols
Solar flux at the surface	reduction	large reduction
ABL solar heating	negligible change	large increase
Sensible heat flux	reduction	large reduction
Evaporation	decrease	decrease
$T_s - T_{2m}$	small decrease	large decrease
ABL temperature	decrease	increase
ABL humidity	small increase (dry-soil) decrease (wet-soil)	decrease
Inversion strength	increase	decrease
ABL growth/collapse	negligible change	later growth/earlier collapse
ABL height	decrease	large increase (dry-soil) small increase (wet-soil)
Entrainment	decrease	increase
Probability of cloud/fog formation	increase (dry-soil) decrease (wet-soil)	decrease

^a Important dependence of perturbation on the soil moisture is also shown.

of ABL and hence reducing the entrainment heating and drying. On the other hand, the increased ABL temperature in the absorbing aerosol case raises the top of ABL in spite of the reduction in the buoyancy flux. For strongly absorbing aerosols, this elevation of the ABL can be substantial and the entrainment heating and drying increase.

[54] The combination of the reduced surface evaporation and the changed entrainment drying determines the sign and magnitude of the perturbation of water vapor in the ABL. For purely scattering aerosols the entrainment drying decreases, compensating (in the wet-soil case) or overcompensating (in the dry-soil case) the reduction in the surface evaporation. For absorbing aerosols, on the other hand, the increased entrainment drying along with the reduced surface evaporation decreases the ABL moisture. Thus changes in the relative humidity depend on the aerosol absorption and soil moisture. The decrease of the RH with absorbing aerosol decreases the probability of formation of clouds in the boundary layer, hence causing an additional warming through cloud-feedback effects.

[55] Sensitivity tests show that the perturbation in the evolution of ABL can be significantly different if some of the absorbing aerosol has been elevated above the ABL, such as smoke from biomass burning or mineral aerosol from a dust storm. For such events, the strength of capping inversion increases because of the significant warming of overlying air, lowering the top of the ABL. The resultant decrease in the entrainment heating also cools the ABL. The reduced entrainment drying can exceed the reduction in the surface evaporation, moistening the ABL. Therefore its RH increases significantly, leading to an increase in the probability of formation of boundary layer clouds.

[56] The radiative effects of aerosols on the evolution of the ABL are sensitive to the optical depth, the single-scattering albedo, and the vertical distribution of aerosols, making it important to characterize these factors [Penner *et al.*, 1994]. In this context, an integration of ground-based observations, satellite measurements, and model simulations would be extremely useful. The in situ aircraft measurements and lidar observations are needed to track the vertical distribution of aerosols. In addition, a thorough investigation of the dependence of aerosol optical properties on the RH is essential to quantifying the RH-feedback effect.

[57] The utilization of the high-resolution ABL model in this study simulates effectively the responses of important ABL processes to the radiative perturbation, including surface heat release, surface evaporation, turbulent mixing, and entrainment. The results here can facilitate the interpretation of complex three-dimensional simulations. On the other hand, the aerosol-radiation-ABL interactions are extremely complex. The 1-D model used here can represent ABLs only for dry subsiding regions such as subtropical highs, and the conclusions may change substantially for other climatic regions. Additional studies are needed, including the development and implementation of appropriate parameterizations of condensation and precipitation processes to investigate cloud feedback processes. In addition, the effect of land cover requires a more sophisticated land/vegetation model. Finally, changes in the ABL dynamics could influence the formation and evolution of photochemical smog. A comprehensive study of combined dynamical and photo-

chemical effects is needed to evaluate the impacts of aerosols on the smog.

[58] **Acknowledgments.** We are grateful to Michael Ek of Oregon State University for providing and helping with the CAPS model. We thank Kuo-Nan Liou at University of California, Los Angeles, for providing the Fu-Liou radiation code. The authors also appreciate valuable comments and suggestions from William Chameides and Yongqiang Liu of Georgia Institute of Technology and C. M. Liu of National Taiwan University. Comments from two anonymous reviewers are gratefully acknowledged. The research was supported by NASA grant NAG5-3844 for the China-MAP project and DOE grant DE-FG02-01ER63198.

References

- Ackerman, A. S., O. B. Toon, D. E. Stevens, A. J. Heymsfield, V. Ramanathan, and E. J. Welton, Reduction of tropical cloudiness by soot, *Science*, **288**, 1042–1047, 2000.
- Albrecht, B. A., Aerosols, cloud microphysics, and fractional cloudiness, *Science*, **245**, 1227–1230, 1989.
- Boucher, O., et al., Intercomparison of models representing direct short-wave radiative forcing by sulfate aerosols, *J. Geophys. Res.*, **103**, 16,979–16,998, 1998.
- Chameides, W. L., et al., A case study of the effects of atmospheric aerosols and regional haze on agriculture: An opportunity to enhance crop yields in China through emission controls?, *Proc. Natl. Acad. Sci.*, **96**(24), 13,626–13,633, 1999.
- Chang, S., D. Hahn, C.-H. Yang, D. Norquist, and M. Ek, Validation study of the CAPS Model land surface scheme using the 1987 Cabauw/PILPS dataset, *J. Appl. Meteorol.*, **38**, 405–422, 1999.
- Charlson, R. J., S. E. Schwartz, J. H. Hales, R. D. Cess, J. A. Coakley Jr., J. E. Hansen, and D. J. Hofmann, Climate forcing by anthropogenic aerosols, *Science*, **255**, 423–430, 1992.
- Ching, J. K. S., S. T. Shipley, and E. V. Browell, Evidence for cloud venting of mixed layer ozone and aerosols, *Atmos. Environ.*, **22**, 225–242, 1988.
- Chylek, P., G. Videen, D. Ngo, R. G. Pinnick, and J. D. Klett, Effect of black carbon on the optical properties and climate forcing of sulfate aerosols, *J. Geophys. Res.*, **100**, 16,325–16,332, 1995.
- Coakley, J. A., Jr., R. D. Cess, and F. B. Yurevich, The effect of tropospheric aerosols on the Earth's radiation budget: A parameterization for climate models, *J. Atmos. Sci.*, **40**, 116–138, 1983.
- d'Almeida, G. A., P. Koepke, and E. P. Shettle, *Atmospheric Aerosols: Global Climatology and Radiative Characteristics*, 561 pp., A. Deepak, Hampton, Va., 1991.
- Ek, M., and L. Mahrt, A formulation for boundary-layer cloud cover, *Ann. Geophys.*, **9**, 716–724, 1991a.
- Ek, M., and L. Mahrt, *OSU 1-D PBL Model: User's Guide*, 108 pp., Oregon State Univ., Corvallis, 1991b.
- Ek, M., and L. Mahrt, Daytime evolution of relative humidity at the boundary layer top, *Mon. Weather Rev.*, **122**, 2709–2721, 1994.
- Foucart, Y., B. Bonnel, G. Bogniez, J. C. Buriez, L. Smith, J. J. Morcrette, and A. Cerf, Observations of Saharan aerosol: Results of ECLATS field experiment, II, Broad-band radiative characteristics of the aerosol and vertical flux divergence, *J. Clim. Appl. Meteorol.*, **26**, 38–53, 1987.
- Fu, Q., and K.-N. Liou, On the correlated k-distribution method for radiative transfer in nonhomogeneous atmospheres, *J. Atmos. Sci.*, **49**, 2139–2156, 1992.
- Fu, Q., and K.-N. Liou, Parameterization of the radiative properties of cirrus clouds, *J. Atmos. Sci.*, **50**, 2008–2025, 1993.
- Fu, Q., K.-N. Liou, M. C. Cribb, T. P. Charlock, and A. Grossman, Multiple scattering parameterization in thermal infrared radiative transfer, *J. Atmos. Sci.*, **54**, 2799–2812, 1997.
- Garratt, J. R., *The Atmospheric Boundary Layer*, 316 pp., Cambridge Univ. Press, New York, 1992.
- Garratt, J. R., A. B. Pittock, and K. Walsh, Response of the atmospheric boundary layer and soil layer to a high altitude, dense aerosol cover, *J. Appl. Meteorol.*, **29**, 35–52, 1990.
- Hansen, J., M. Sato, and R. Ruedy, Long-term changes of the diurnal temperature cycle: Implications about mechanisms of global climate change, *Atmos. Res.*, **37**, 175–209, 1995.
- Hansen, J., M. Sato, and R. Ruedy, Radiative forcing and climate response, *J. Geophys. Res.*, **102**, 6831–6864, 1997.
- Heintzenberg, J., R. J. Charlson, A. D. Clarke, C. Liousse, V. Ramaswamy, K. P. Shine, M. Wendisch, and G. Helas, Measurements and modeling of aerosol single-scattering albedo: Progress, problems and prospects, *Beitr. Phys. Atmos.*, **70**, 249–263, 1997.
- Hillel, D., *Introduction to Soil Physics*, 364 pp., Academic, San Diego, Calif., 1982.

- Holtzlag, A. A. M., and B. Boville, Local versus nonlocal boundary-layer diffusion in a global climate model, *J. Clim.*, *6*, 1825–1842, 1993.
- Holtzlag, A. A. M., and M. Ek, The simulation of surface fluxes and boundary-layer development over the pine forest in HAPEX-MOBILHY, *J. Appl. Meteorol.*, *35*, 202–213, 1996.
- Holtzlag, A. A. M., and C.-H. Moeng, Eddy diffusivity and countergradient transport in the convective atmospheric boundary layer, *J. Atmos. Sci.*, *48*, 1690–1698, 1991.
- Holtzlag, A. A. M., and A. P. van Ulden, A simple scheme for daytime estimates of the surface fluxes from routine weather data, *J. Clim. Appl. Meteorol.*, *22*, 517–529, 1983.
- Holtzlag, A. A. M., E. I. F. de Bruijn, and H.-L. Pan, A high resolution air mass transformation model for short-range weather forecasting, *Mon. Weather Rev.*, *118*, 1561–1575, 1990.
- Hong, S. Y., and H.-L. Pan, Nonlocal boundary layer vertical diffusion in a medium-range forecast model, *Mon. Weather Rev.*, *124*, 2322–2339, 1996.
- Intergovernmental Panel on Climate Change (IPCC), Radiative forcing of climate change, in *Climate Change 1994: Radiative Forcing of Climate Change and an Evaluation of the IPCC IS92 Emission Scenarios*, pp. 131–162, Cambridge Univ. Press, New York, 1994.
- IPCC, Radiative forcing of climate change, in *Climate Change 1995: The Science of Climate Change*, pp. 103–118, Cambridge Univ. Press, New York, 1996.
- Kiehl, J. T., and B. P. Briegleb, The relative role of sulfate aerosols and greenhouse gases in climate forcing, *Science*, *260*, 311–314, 1993.
- Mahrt, L., and H.-L. Pan, A two-layer model of soil hydrology, *Boundary Layer Meteorol.*, *29*, 1–20, 1984.
- Nemesure, S., R. Wagener, and S. E. Schwartz, Direct shortwave forcing of climate by anthropogenic sulfate aerosol: Sensitivity to particle size, composition and relative humidity, *J. Geophys. Res.*, *100*, 26,105–26,116, 1995.
- Penner, J. E., R. E. Dickinson, and C. A. O'Neill, Effects of aerosol from biomass burning on the global radiation budget, *Science*, *256*, 1432–1434, 1992.
- Penner, J. E., R. J. Charlson, J. M. Hales, N. Laulainen, R. Leifer, T. Novakov, J. Ogren, L. F. Radke, S. E. Schwartz, and L. Travis, Quantifying and minimizing uncertainty of climate forcing by anthropogenic aerosols, *Bull. Am. Meteorol. Soc.*, *75*, 375–400, 1994.
- Russell, P. B., J. M. Livingston, P. Hignett, S. Kinne, J. Wond, A. Chien, R. Bergstrom, P. Durkee, and P. V. Hobbs, Aerosol-induced radiative flux changes off the United States mid-Atlantic coast: Comparison of values calculated from sunphotometer and in situ data with those measured by airborne pyranometer, *J. Geophys. Res.*, *104*, 2289–2307, 1999.
- Stenchikov, G. L., and A. Robock, Diurnal asymmetry of climatic response to increased CO₂ and aerosols: Forcing and feedbacks, *J. Geophys. Res.*, *100*, 26,211–26,227, 1995.
- Trenberth, K. E., (Ed.), *Climate System Modeling*, 788 pp., Cambridge Univ. Press, New York, 1992.
- Troen, I., and L. Mahrt, A simple model of the atmospheric boundary layer: Sensitivity to surface evaporation, *Boundary Layer Meteorol.*, *37*, 129–148, 1986.
- Twomey, S., The influence of pollution on the shortwave albedo of clouds, *J. Atmos. Sci.*, *34*, 1149–1152, 1977.
- Yu, H., Radiative effects of aerosols on the environment in China, Ph.D. dissertation, 226 pp., Ga. Inst. of Technol., July 2000.

R. Dickinson and H. Yu, School of Earth and Atmospheric Sciences, Georgia Institute of Technology, 221 Bobby Dodd Way, Atlanta, GA 30332, USA. (robed@eas.gatech.edu; yu@breeze.eas.gatech.edu)
 S. C. Liu, Institute of Earth Sciences, Academia Sinica, P.O. Box 1-55, Nankang, Taipei, Taiwan, 11529. (shawliu@earth.sinica.edu.tw)